



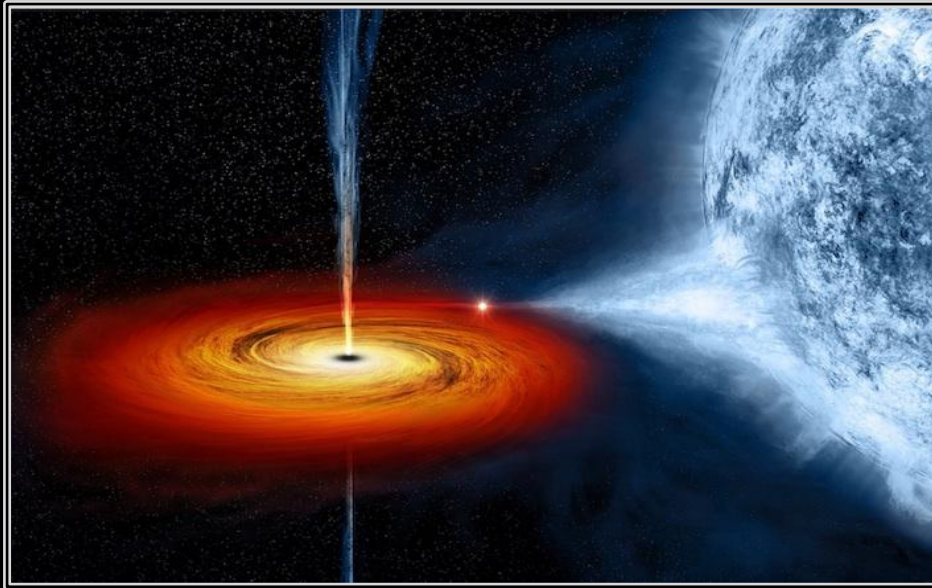
Modeling of Wind -fed accretion in HMXBs using GRMHD code

-Ishika Palit

Supervisor : Prof. Agnieszka Janiuk

Date : 20.10.2020

{ RAGtime 22 }



Plan of Talk:

➡ **Introduction to X-ray binaries**

➡ **Wind fed accretion in Cygnus X-1**

➡ **GRMHD simulation (HARM)**

➡ **Results and outcomes**

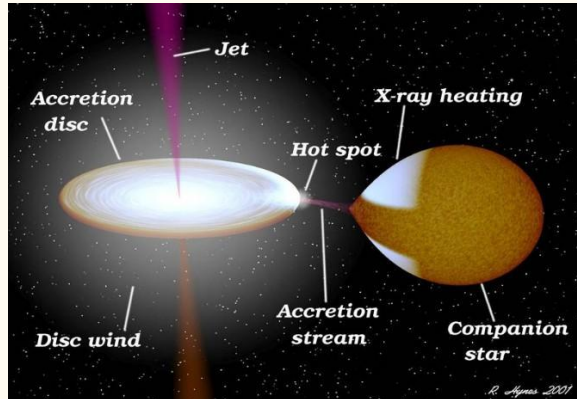
X-ray Binaries

X-ray Binary systems contain one normal star and one collapsed star that orbit around their common center of mass.

(low-mass X-ray binaries, LMXBs)

(high-mass X-ray binaries, HMXBs)

The X-rays are produced as material from the companion star is drawn to the compact object either through



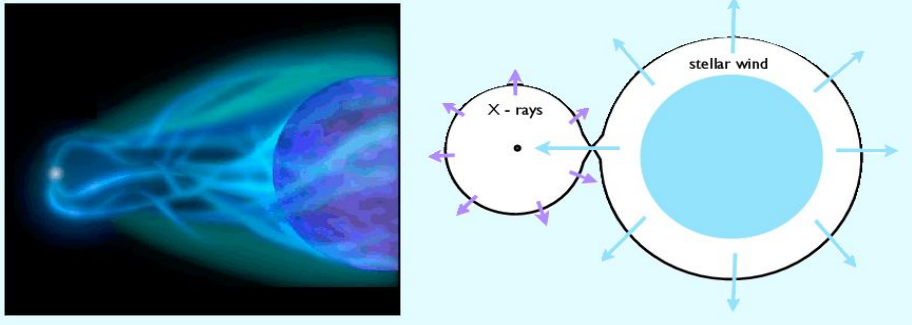
- ◆ Roche-lobe overflow into an accretion disk
- ◆ Direct impact of a stellar wind onto the compact object

Scorpius X-1 and Cygnus X-1 were first X-ray sources to be discovered in the constellations of Scorpius and Cygnus respectively.

HMXBs are brighter in X-rays not just because of accretion disk but also due to presence of extremely hot corona.

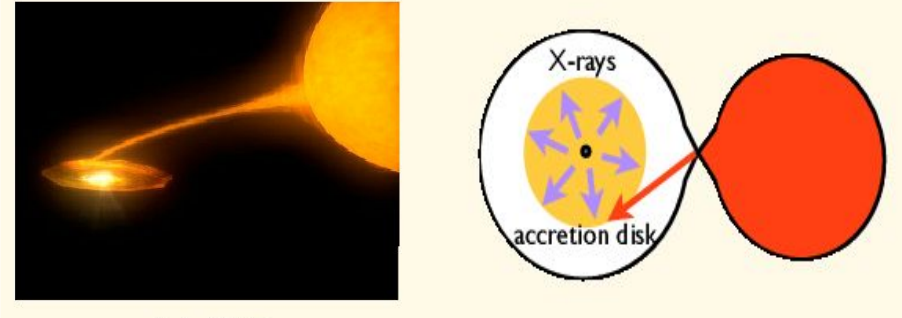
[credits- NASA/R. Hynes]

HMXB's



- High Mass companion star ($\geq 10 M_{\odot}$), mostly O or B type stars
- Mostly Stellar wind accretion
- If collapsed star less massive than companion then remains as a binary system.
- Higher energy X-ray emission.

LMXB's



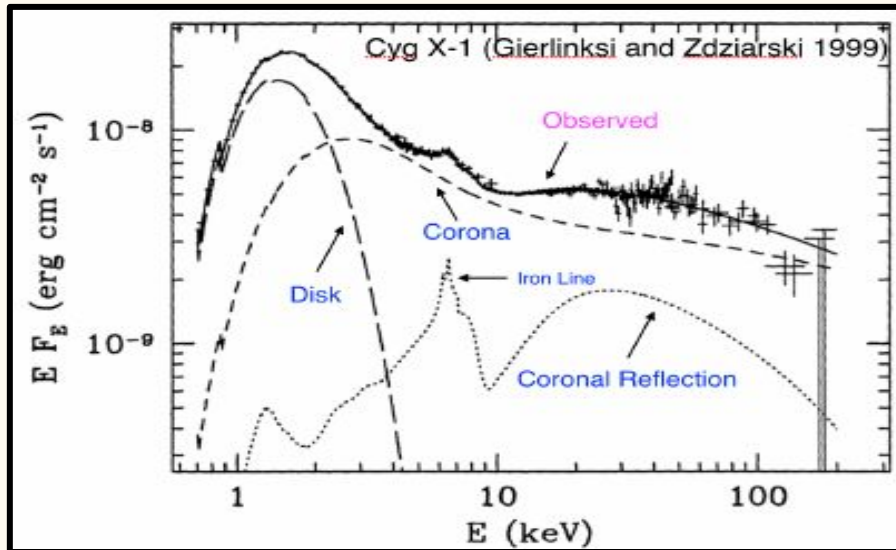
- Low Mass companion star ($\leq 1 M_{\odot}$), mostly K or M type star or a white dwarf
- Roche Lobe overflow
- The mass transfer on to the compact object is much slower and more controlled.
- They emit lower energy X-rays.

Cygnus X-1: Spectra & wind properties

X-ray binary system:

Cygnus X-1 – Black hole $\sim (20 M_{\odot})$

HDE-226868 – Supergiant star ($\sim 40 M_{\odot}$)



Focused stellar wind:

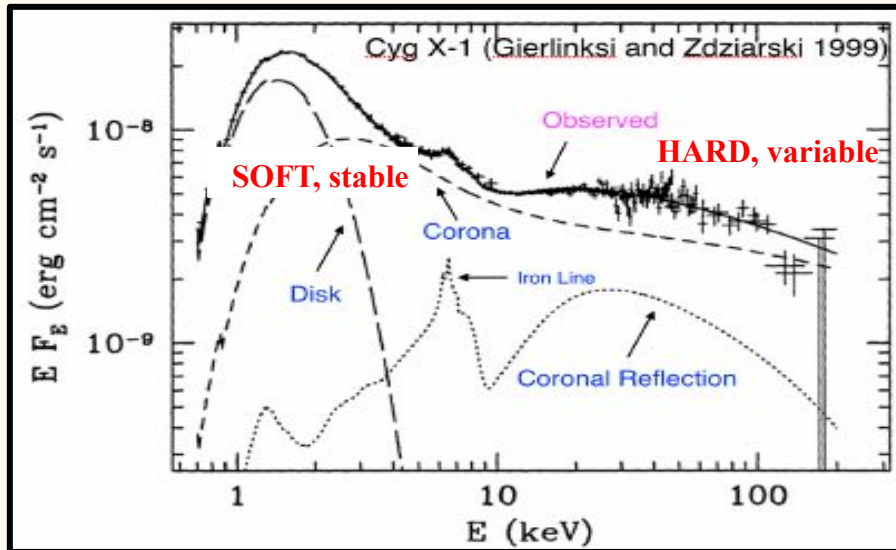
- ◆ Important variability component due to the variable (clumpy) stellar wind from the companion.
- ◆ Winds are powered by radiation pressure acting through absorption in spectral lines (CAK mechanism).
- ◆ Perturbations present in the wind causing variations in the parameters of the flow such as density, velocity and temperature, which compress the gas into small, cold, and over-dense structures, often referred to as “clumps”.
- ◆ These clumps are stated responsible for the observed absorption dips (i.e the lower flux) in the Hard State spectra

Cygnus X-1: Spectra & wind properties

X-ray binary system:

Cygnus X-1 – Black hole $\sim (20 M_{\odot})$

HDE-226868 – Supergiant star ($\sim 40 M_{\odot}$)



Focused stellar wind:

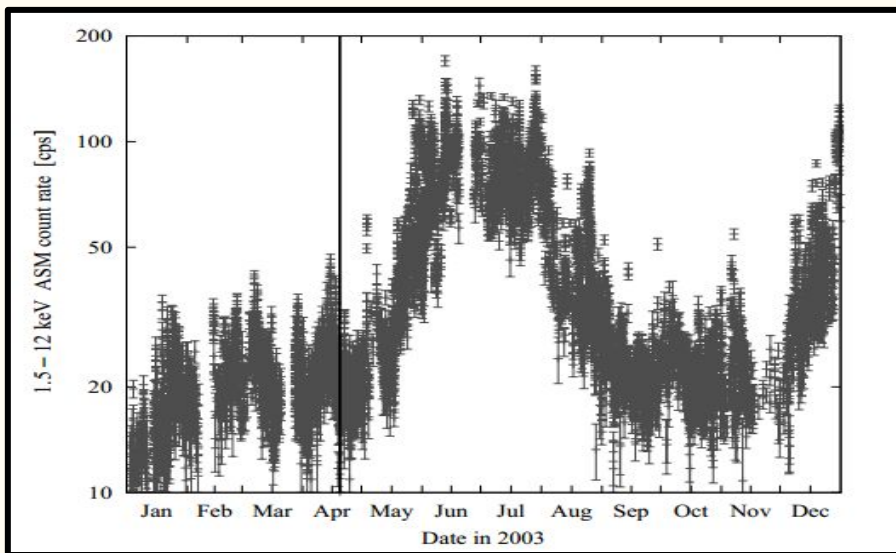
- ◆ Important variability component due to the variable (clumpy) stellar wind from the companion.
- ◆ Winds are powered by radiation pressure acting through absorption in spectral lines (CAK mechanism).
- ◆ Perturbations present in the wind causing variations in the parameters of the flow such as density, velocity and temperature, which compress the gas into small, cold, and over-dense structures, often referred to as “clumps”.
- ◆ These clumps are stated responsible for the observed absorption dips (i.e the lower flux) in the Hard State spectra

Cygnus X-1: Spectra & wind properties

X-ray binary system:

Cygnus X-1 – Black hole $\sim (20 M_{\odot})$

HDE-226868 – Supergiant star ($\sim 40 M_{\odot}$)



Focused stellar wind:

- ◆ Important variability component due to the variable (clumpy) stellar wind from the companion.
- ◆ Winds are powered by radiation pressure acting through absorption in spectral lines (CAK mechanism).
- ◆ Perturbations present in the wind causing variations in the parameters of the flow such as density, velocity and temperature, which compress the gas into small, cold, and over-dense structures, often referred to as “clumps”.
- ◆ These clumps are stated responsible for the observed absorption dips (i.e the lower flux) in the Hard State spectra

(Hanke, M. et. al , 2009, ApJ)

Cygnus X-1: Spectra & wind properties

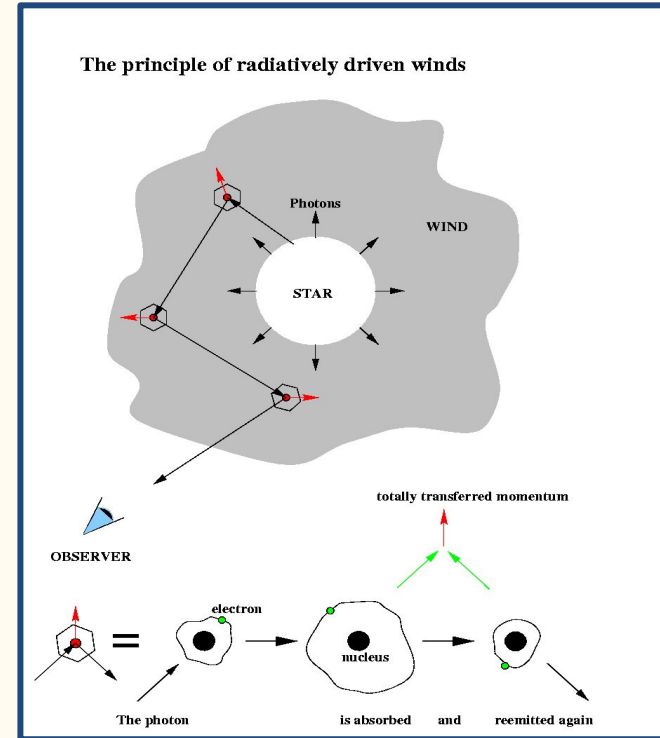
Stellar wind driving mechanism : **Radiation-driven Winds**

Wind model : **Line-driven wind model**
CAK [Castor, Abbott & Klein, 1975]
formalism

In hot stars:

absorption by spectral lines of atoms

Properties are high velocities and high mass loss

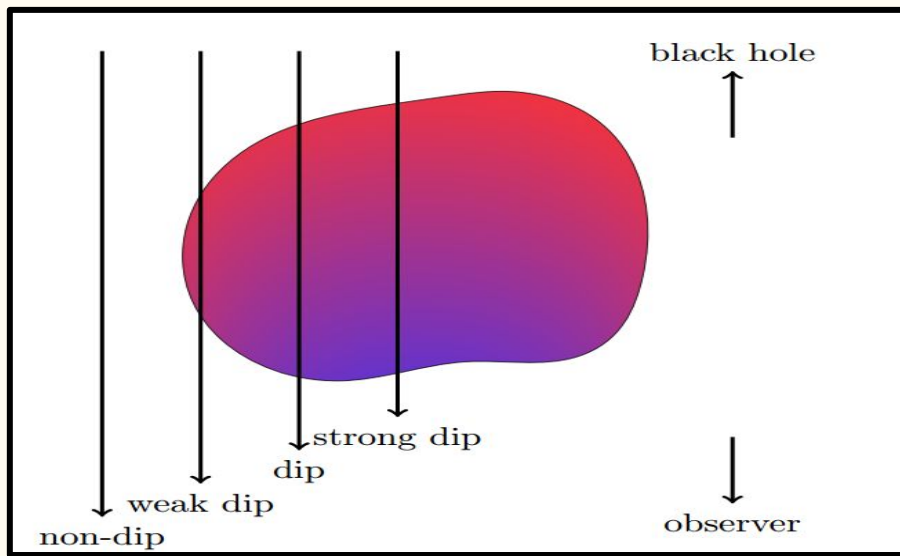


Cygnus X-1: Spectra & wind properties

X-ray binary system:

Cygnus X-1 – Black hole $\sim (20 M_{\odot})$

HDE-226868 – Supergiant star $(\sim 40 M_{\odot})$



Focused stellar wind:

- ◆ Important variability component due to the variable (clumpy) stellar wind from the companion.
- ◆ Winds are powered by radiation pressure acting through absorption in spectral lines (CAK mechanism).
- ◆ Perturbations present in the wind causing variations in the parameters of the flow such as density, velocity and temperature, which compress the gas into small, cold, and over-dense structures, often referred to as “clumps”.
- ◆ These clumps are stated responsible for the observed absorption dips (i.e the lower flux) in the Hard State spectra

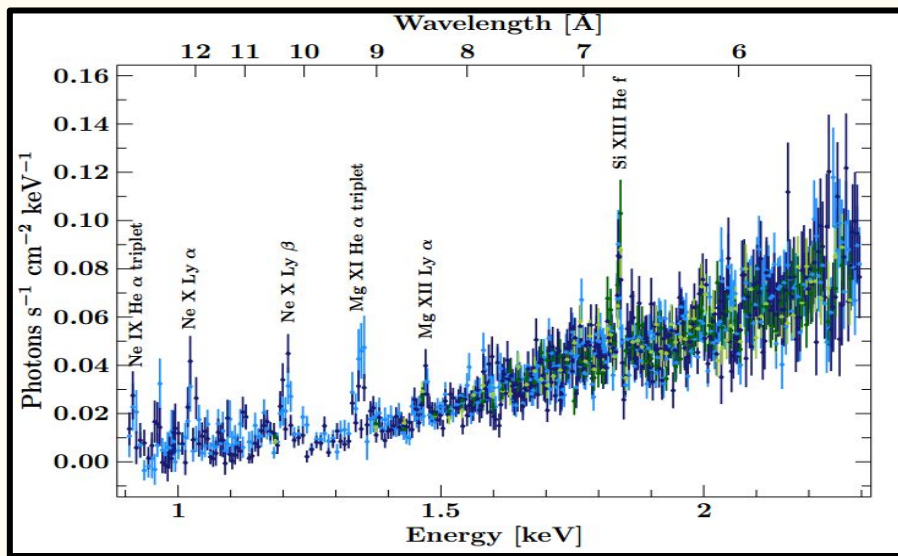
(Hirsch, M. et. al , 2019, A&A)

Cygnus X-1: Spectra & wind properties

X-ray binary system:

Cygnus X-1 – Black hole $\sim (20 M_{\odot})$

HDE-226868 – Supergiant star ($\sim 40 M_{\odot}$)



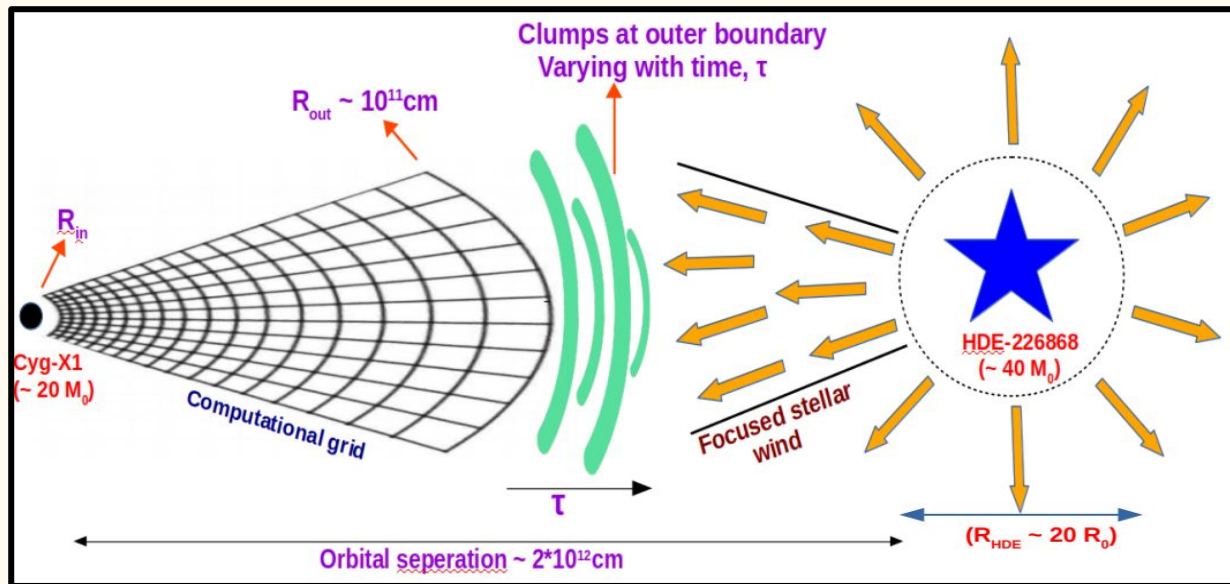
Focused stellar wind:

- ◆ Important variability component due to the variable (clumpy) stellar wind from the companion.
- ◆ Winds are powered by radiation pressure acting through absorption in spectral lines (CAK mechanism).
- ◆ Perturbations present in the wind causing variations in the parameters of the flow such as density, velocity and temperature, which compress the gas into small, cold, and over-dense structures, often referred to as “clumps”.
- ◆ These clumps are stated responsible for the observed absorption dips (i.e the lower flux) in the Hard State spectra

(Hirsch, M. et. al , 2019, A&A)

Our model set-up

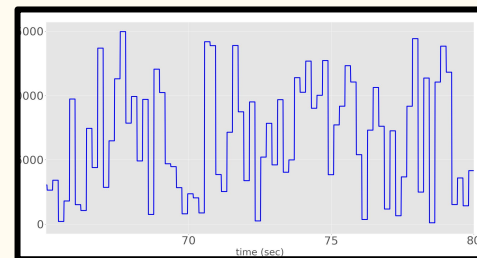
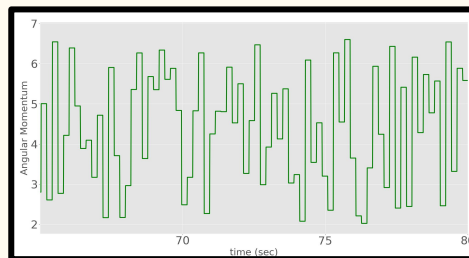
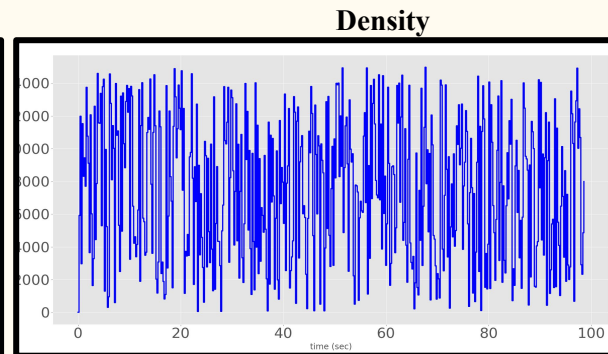
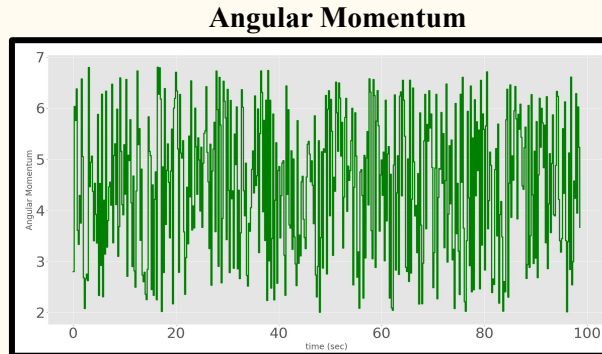
- ◆ The prescription of density at the outer boundary is estimated from the observed data [$\rho_{\max} = 10^{-15} \text{ g cm}^{-3}$ (15000 [M]) , $\rho_{\min} = 0 \text{ g cm}^{-3}$]
- ◆ The choice for angular momentum is motivated by the values of angular momentum at marginally stable orbit, $\lambda_{\text{ms}} = 3.67 \text{ GM}_{\text{BH}}/c^2$ and at marginally bound orbit, $\lambda_{\text{mb}} = 4\text{GM}_{\text{BH}}/c^2$ (Das & Chakrabarti 1999).
- ◆ We implement a function generating values between the prescribed maximum and minimum amplitude of density & angular momentum.



(Ref: I.Palit et.al, 2020, ApJ)

Our model set-up

- ◆ The prescription of density at the outer boundary is estimated from the observed data [$\rho_{\max} = 10^{-15} \text{ g cm}^{-3}$ (15000 [M]) , $\rho_{\min} = 0 \text{ g cm}^{-3}$]
- ◆ The choice for angular momentum is motivated by the values of angular momentum at marginally stable orbit, $\lambda_{\text{ms}} = 3.67 \text{ GM}_{\text{BH}}/c^2$ and at marginally bound orbit, $\lambda_{\text{mb}} = 4\text{GM}_{\text{BH}}/c^2$ (Das & Chakrabarti 1999).
- ◆ We implement a function generating values between the prescribed maximum and minimum amplitude of density & angular momentum.



$$(\lambda_{\max} = 2.0[M], \lambda_{\min} = 6.8 [M])$$

(Ref: I.Palit et.al, 2020, ApJ)

Initial conditions & shock solution

Initial conditions:

➡ Quasi-spherical distribution of gas, provided by constant specific angular momentum for a non-Keplerian accretion disk.

(Abramowicz & Zurek 1981)

➡ Transonic Accretion - Shock solution (Pressure waves travel with sound speed) , $C_{\text{sound}} = (\text{Pressure} * \text{adiabatic index}) / \text{density}$

➡ Time dependent outer boundary condition

➡ Inviscid, non-magnetized flow

➡ Polytropic Equation of state ($P = K\rho^\gamma$)

Initial conditions & shock solution

Initial conditions:

➡ Quasi-spherical distribution of gas, provided by constant specific angular momentum for a non-Keplerian accretion disk.
(Abramowicz & Zurek 1981)

➡ Transonic Accretion - Shock solution (Pressure waves travel with sound speed) , $C_{\text{sound}} = (\text{Pressure} * \text{adiabatic index}) / \text{density}$

➡ Time dependent outer boundary condition

➡ Inviscid, non-magnetized flow

➡ Polytropic Equation of state ($P = K\rho^\gamma$)

Shock solution:

$$\dot{M} = u\rho r^2 \quad \text{Mass conservation equation}$$

$$u \frac{du}{dr} + \frac{1}{\rho} \frac{dP}{dr} + \frac{d}{dr}(\Phi(r)) = 0 \quad \text{radial momentum equation}$$

$$\epsilon = \frac{1}{2}u^2 + \frac{a^2}{(\gamma-1)} + \frac{\lambda^2}{2}r^2 + \phi = 0 \quad \text{energy conservation equation in steady state}$$

Initial conditions & shock solution

Initial conditions:

➡ Quasi-spherical distribution of gas, provided by constant specific angular momentum for a non-Keplerian accretion disk.
(Abramowicz & Zurek 1981)

➡ Transonic Accretion - Shock solution (Pressure waves travel with sound speed) , $C_{\text{sound}} = (\text{Pressure} * \text{adiabatic index}) / \text{density}$

➡ Time dependent outer boundary condition

➡ Inviscid, non-magnetized flow

➡ Polytropic Equation of state ($P = K\rho^\gamma$)

Shock solution:

$$a_c = \sqrt{\frac{r}{2} \frac{d\phi(r)}{dr} - \frac{\lambda^2}{2r^2}} = \sqrt{\frac{r}{4(r-1)^2} - \frac{\lambda^2}{2r^2}}$$

local sound speed

$$\epsilon = \frac{1}{2}u^2 + \frac{a^2}{(\gamma-1)} + \frac{\lambda^2}{2}r^2 + \phi = 0$$

energy conservation
equation in steady state

Initial conditions & shock solution

Initial conditions:

➡ Quasi-spherical distribution of gas, provided by constant specific angular momentum for a non-Keplerian accretion disk.

(Abramowicz & Zurek 1981)

➡ Transonic Accretion - Shock solution (Pressure waves travel with sound speed) , $C_{\text{sound}} = (\text{Pressure} * \text{adiabatic index}) / \text{density}$

➡ Time dependent outer boundary condition

➡ Inviscid, non-magnetized flow

➡ Polytropic Equation of state ($P = K\rho^\gamma$)

Shock solution:

Critical point, $r_c(\epsilon, \lambda, \gamma)$:

$$\epsilon - \frac{\lambda^2}{2r_c^2} - \frac{\gamma + 1}{2(\gamma - 1)} \left(\frac{r_c}{4(r_c - 1)^2} - \frac{\lambda^2}{2r_c^2} \right) = 0$$

Mach Number (\mathcal{M}) = $\frac{\text{Flow Velocity}}{\text{Local sound speed}}$

(Suková P. et.al, 2015, MNRAS)

(Suková P. et.al, 2017, MNRAS)

(Palit, I. et.al, 2019, MNRAS)

Initial conditions & shock solution

Initial conditions:

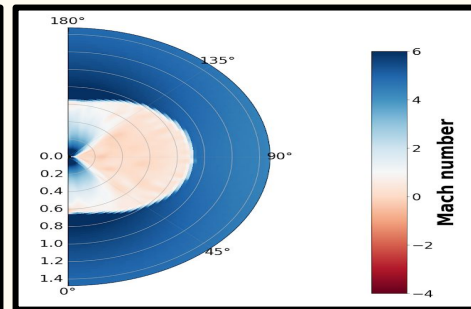
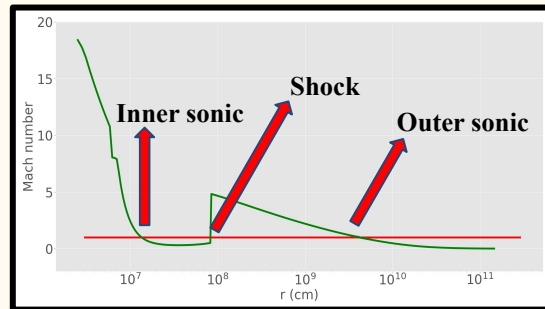
- ➡ Quasi-spherical distribution of gas, provided by constant specific angular momentum for a non-Keplerian accretion disk.
(Abramowicz & Zurek 1981)
- ➡ Time dependent outer boundary condition
- ➡ Inviscid, non-magnetized flow
- ➡ Transonic Accretion - Shock solution (Pressure waves travel with sound speed) , $C_{\text{sound}} = (\text{Pressure} * \text{adiabatic index}) / \text{density}$
- ➡ Polytropic Equation of state ($P = K\rho^\gamma$)

Shock solution:

Critical point, r_c ($\epsilon, \lambda, \gamma$):

$$\epsilon - \frac{\lambda^2}{2r_c^2} - \frac{\gamma + 1}{2(\gamma - 1)} \left(\frac{r_c}{4(r_c - 1)^2} - \frac{\lambda^2}{2r_c^2} \right) = 0$$

Mach Number (M) = $\frac{\text{Flow Velocity}}{\text{Local sound speed}}$



Subsonic ($M < 1$),

Supersonic ($M > 1$)

(Suková P. et.al, 2015, MNRAS)
(Suková P. et.al, 2017, MNRAS)
(Palit, I. et.al, 2019, MNRAS)

HARM

(High Accuracy Relativistic magnetohydrodynamic)

HARM is a conservative shock capturing scheme, for evolving the equations of GRMHD

(developed by C.Gammie et al. 2003)

(Current version of code have many modifications and additions by Prof. Janiuk and group)

Continuity eq :

$$\frac{1}{\sqrt{-g}} \partial_\mu (\sqrt{-g} \rho u^\mu) = 0,$$

**Four-momentum-energy
conservation eq:**

$$\partial_t (\sqrt{-g} T^t_\nu) = -\partial_i (\sqrt{-g} T^i_\nu) + \sqrt{-g} T^\kappa_\lambda \Gamma^\lambda_{\nu\kappa},$$

Induction eq:

$$\partial_t (\sqrt{-g} B^i) = -\partial_j (\sqrt{-g} (b^j u^i - b^i u^j)).$$

**Stress tensor separates into gas and
electromagnetic parts:**

$$\begin{aligned} T^{\mu\nu} &= T_{gas}^{\mu\nu} + T_{EM}^{\mu\nu}, \\ T_{gas}^{\mu\nu} &= \rho h u^\mu u^\nu + p g^{\mu\nu} = (\rho + u + p) u^\mu u^\nu + p g^{\mu\nu}, \\ T_{EM}^{\mu\nu} &= b^2 u^\mu u^\nu + \frac{1}{2} b^2 g^{\mu\nu} - b^\mu b^\nu; b^\mu = u_\nu^* F^{\mu\nu}. \end{aligned}$$

HARM

(High Accuracy Relativistic magnetohydrodynamic)

HARM is a conservative shock capturing scheme, for evolving the equations of GRMHD

(developed by C.Gammie et al. 2003)

(Current version of code have many modifications and additions by Prof. Janiuk and group)

(GRMHD)

Continuity eq :

$$\frac{1}{\sqrt{-g}} \partial_\mu (\sqrt{-g} \rho u^\mu) = 0,$$

**Four-momentum-energy
conservation eq:**

$$\partial_t (\sqrt{-g} T^t_\nu) = -\partial_i (\sqrt{-g} T^i_\nu) + \sqrt{-g} T^\kappa_\lambda \Gamma^\lambda_{\nu\kappa},$$

Induction eq:

~~$$\partial_t (\sqrt{-g} B^i) = -\partial_j (\sqrt{-g} (\delta^i_j \alpha - \delta^j_i \alpha^*)).$$~~

**Stress tensor separates into gas and
electromagnetic parts:**

~~$$\begin{aligned} T^{\mu\nu} &= T_{gas}^{\mu\nu} + T_{EM}^{\mu\nu}, \\ T_{gas}^{\mu\nu} &= \rho h u^\mu u^\nu + p g^{\mu\nu} = (\rho + u + p) u^\mu u^\nu + p g^{\mu\nu}, \\ T_{EM}^{\mu\nu} &= b^2 u^\mu u^\nu + \frac{1}{2} b^2 g^{\mu\nu} - b^\mu b^\nu, \quad b^\mu = \alpha^{-1} F^{\mu\nu} \end{aligned}$$~~

Numerical Scheme:

Specification of geometric quantities

- ➡ In 2D, need to evaluate $g^{\mu\nu}$, $g_{\mu\nu}$ & $\sqrt{-g}$ at four points in every grid zone (center, two faces, and one corner) and $T^\mu_{\nu\lambda}$ at the zone center.
- ➡ Difficult to accurately encode analytic expressions for all these quantities so only be provided for $g_{\mu\nu}$

For ex- The metric connection obtained to sufficient accuracy by numerical differentiation of the metric.

$$\Gamma^i_{kl} = \frac{1}{2} g^{im} \left(\frac{\partial g_{mk}}{\partial x^l} + \frac{\partial g_{ml}}{\partial x^k} - \frac{\partial g_{kl}}{\partial x^m} \right) = \frac{1}{2} g^{im} (g_{mk,l} + g_{ml,k} - g_{kl,m}),$$

Density and internal energy floors

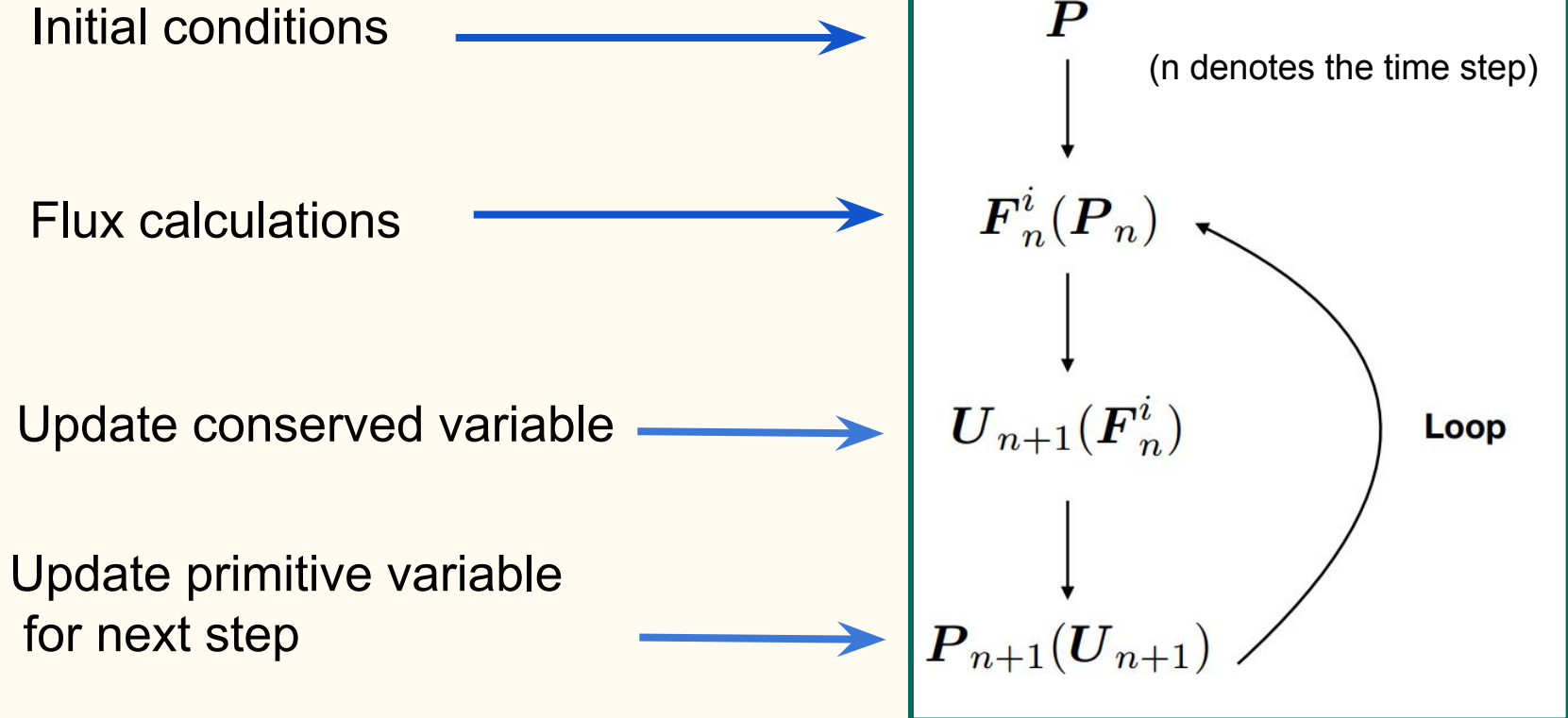
- ➡ Negative densities and internal energies are forbidden by the GRMHD equations
- ➡ Negative internal energies are common in numerical integrations with large density or pressure contrast.
- ➡ Prevent this by introducing “ floor ” values for the density and internal energy.

Numerical Scheme:

- ➡ 2-D simulations are axisymmetric, i.e. the derivatives of quantities in ϕ -direction are neglected (however, velocity field and magnetic field vectors still have all the 3 components)
- ➡ HARM solves GRMHD equations in modified version of Kerr-Schild coordinate system (KS) rather than Boyer-Lindquist coordinates.
- ➡ The integrated equations are of the form:

$$\partial_t U(\mathbf{P}) = -\partial_i F^i(\mathbf{P}) + S(\mathbf{P}),$$

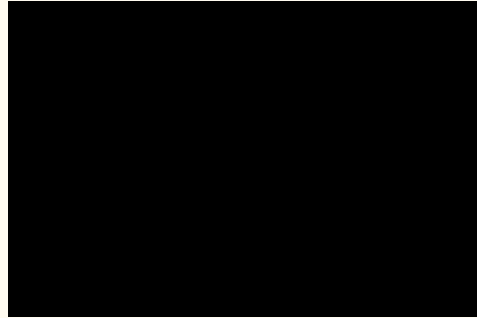
Numerical Scheme:



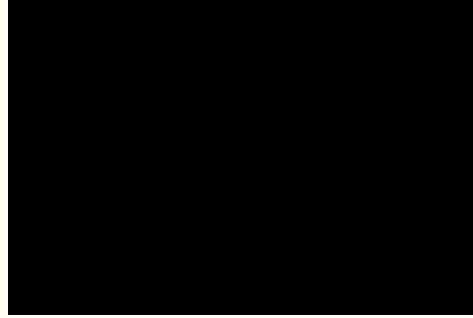
Numerical Scheme:

- ➡ 2-D simulations are axisymmetric, i.e. the derivatives of quantities in ϕ -direction are neglected (however, velocity field and magnetic field vectors still have all the 3 components)
- ➡ HARM solves GRMHD equations in modified version of Kerr-Schild coordinate system (KS) rather than Boyer-Lindquist coordinates.
- ➡ The integrated equations are of the form:
$$\partial_t U(P) = -\partial_i F^i(P) + S(P),$$
- ➡ Choices added for outer boundary conditions:
 - 1] Bound – Default (No mass inflow or outflow)
 - 2] Bound - Fixed (I. Palit et.al, 2019)
 - 3] Bound - Time (I. Palit et.al, 2020)

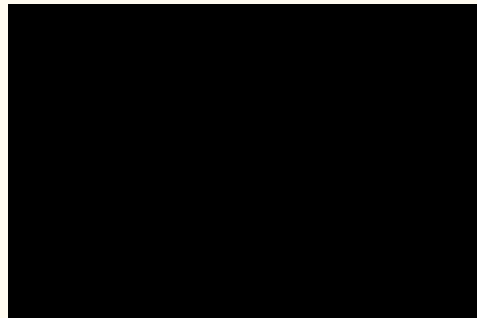
Results: Effects due to time dependent outer boundary conditions



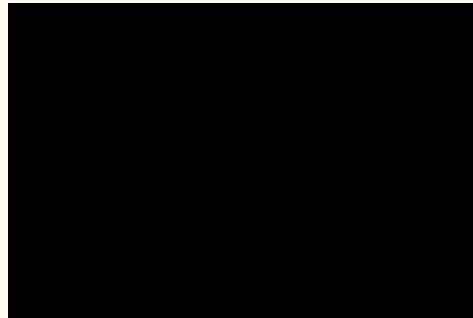
Angular Momentum



Density

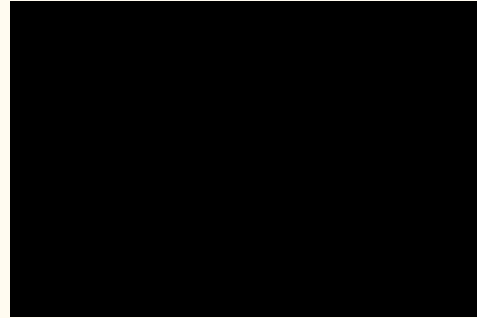


Mach number

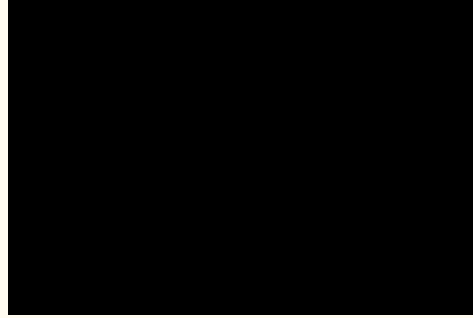


Radial Velocity

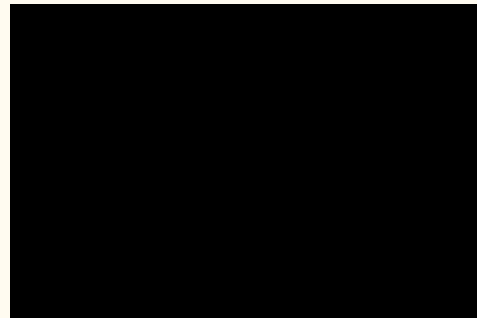
Results: Effects due to time dependent outer boundary conditions



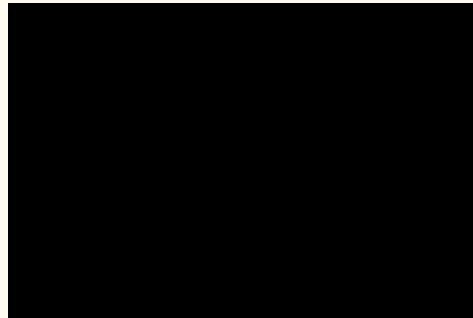
Angular Momentum



Density

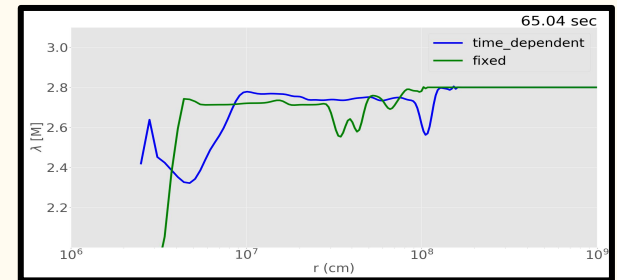
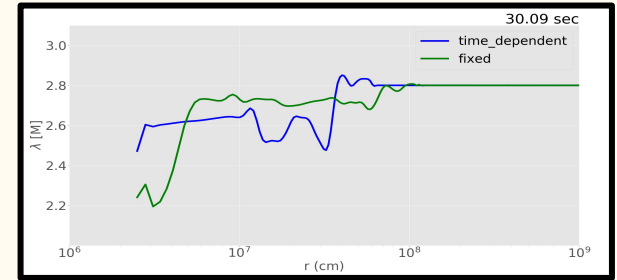


Mach number



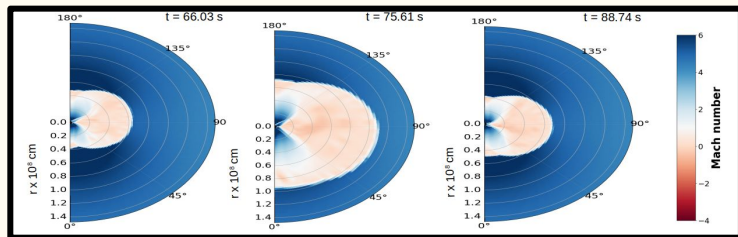
Radial Velocity

Angular momentum profile close to Horizon

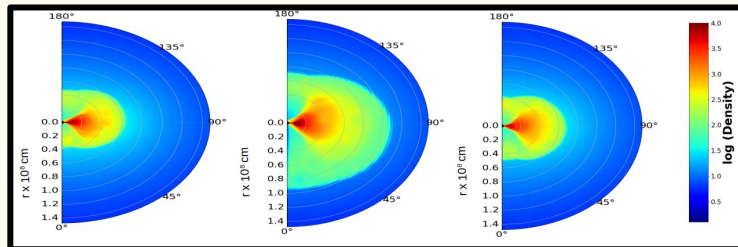


Results: 2D snapshots and Shock evolution

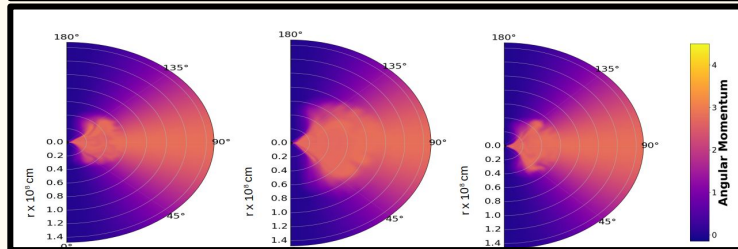
Mach Number



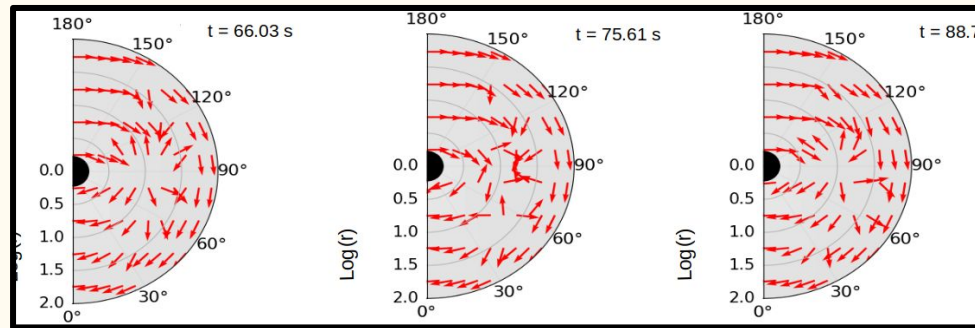
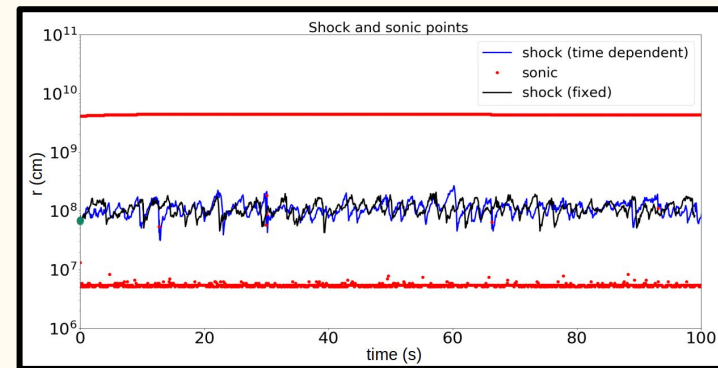
Density



Angular Momentum

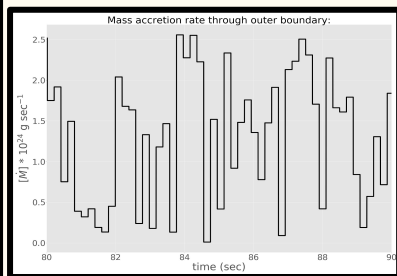
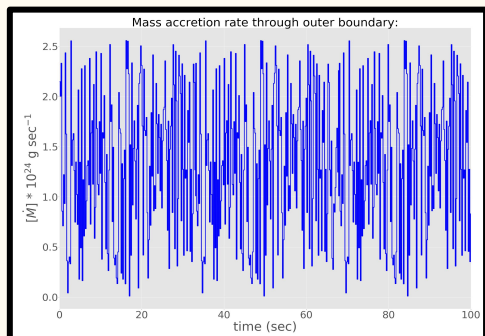
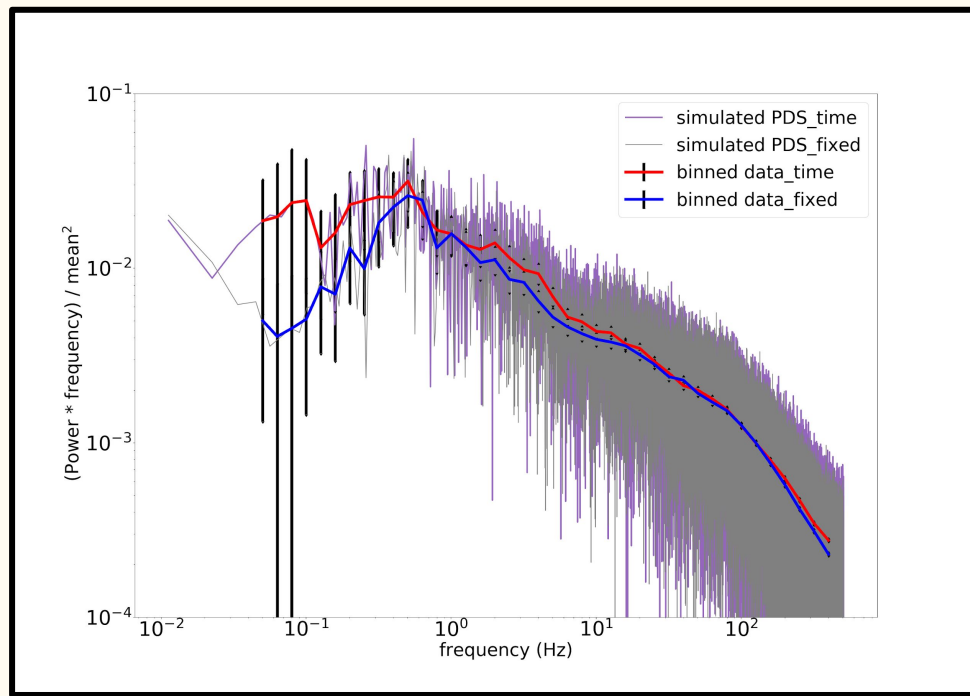
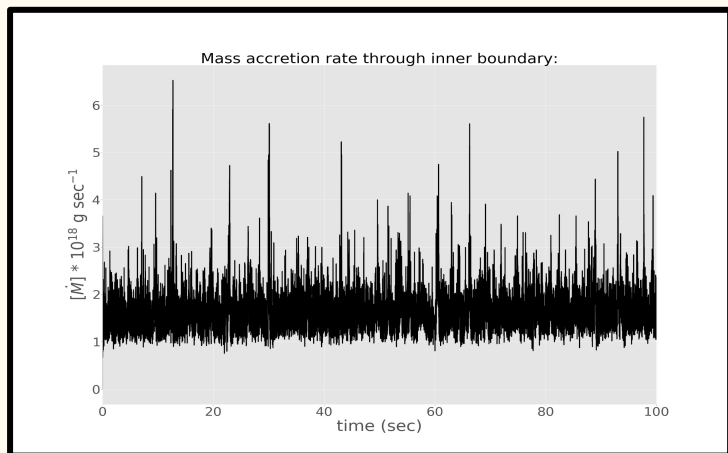


Shock evolution

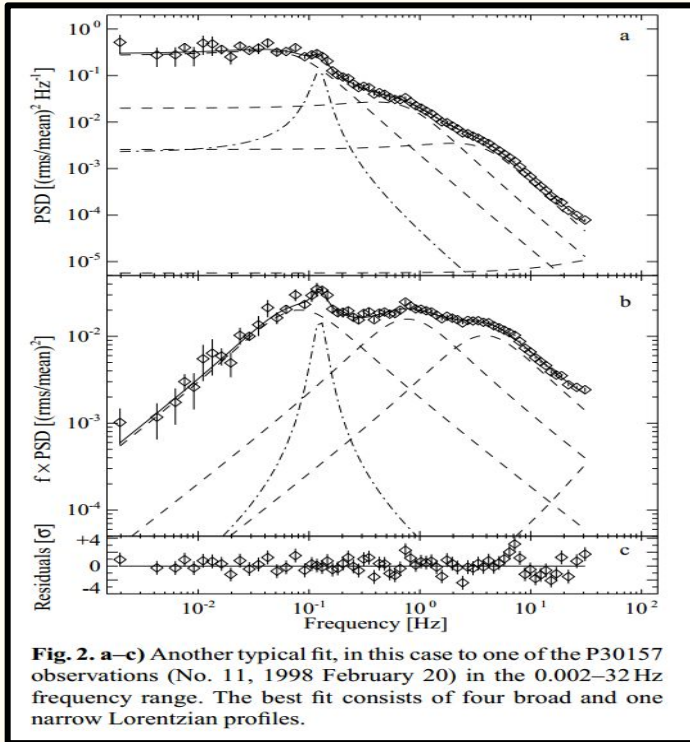


Velocity field lines

Results: Mass accretion rate & Power Density Spectra (PDS)

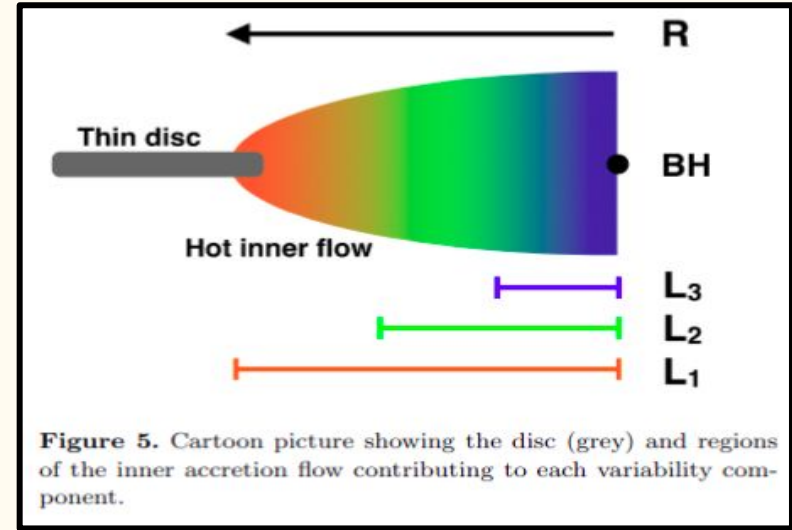


Comparison to observational Data



Pottschmidt et al. (2003)

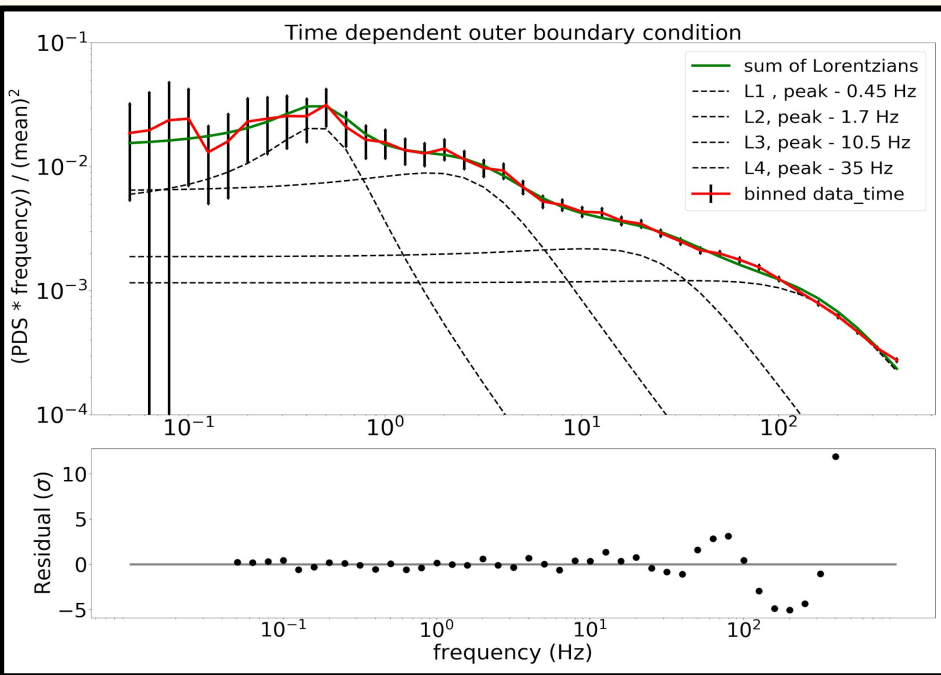
$$L(f) = \pi^{-1} \frac{2R^2 Q f_r}{f_r^2 + 4Q^2 (f - f_r)^2}$$



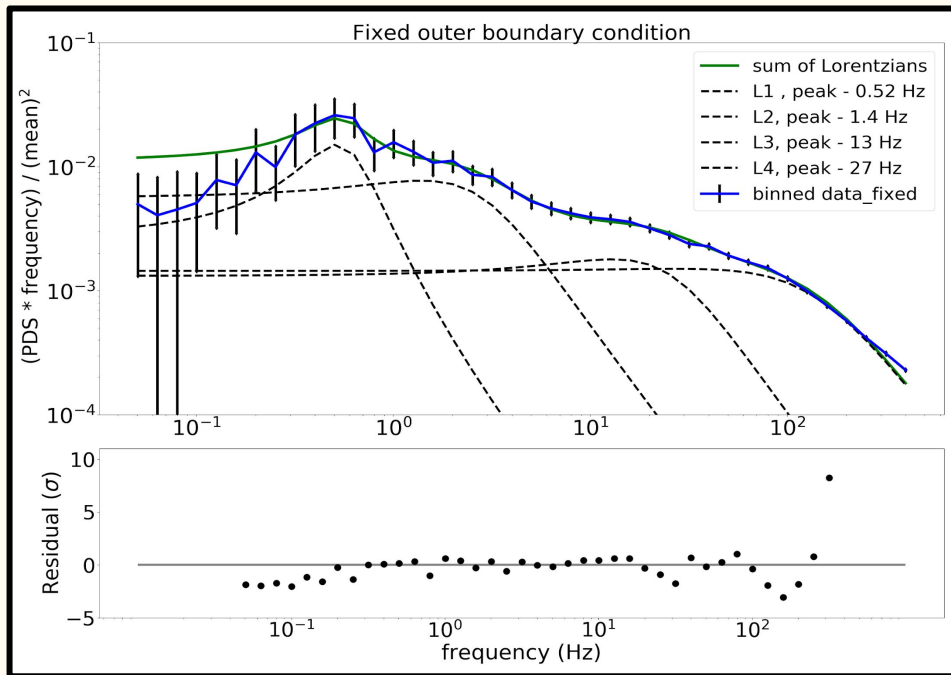
Axelsson & Done (2018)

Results: Lorentzian Fitting

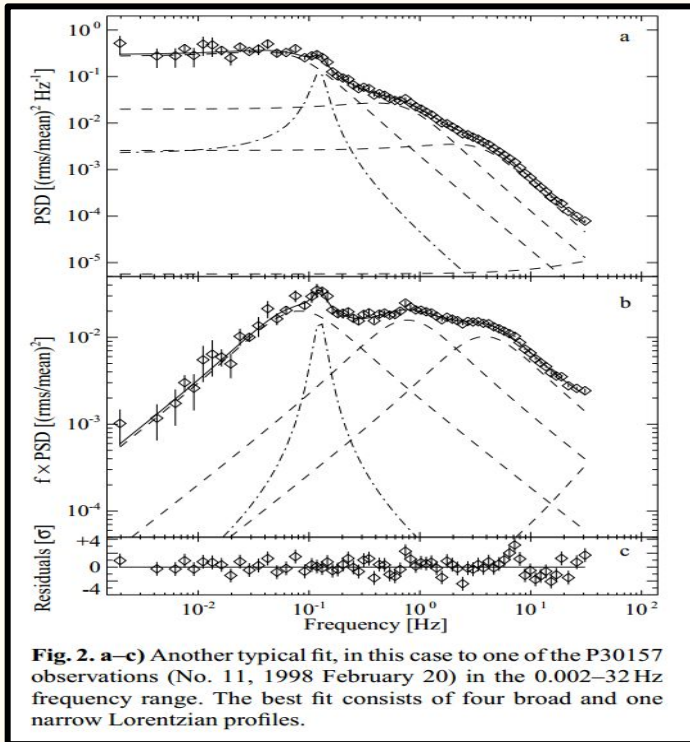
Reduced χ^2 : 8.84



Reduced χ^2 : 15.25



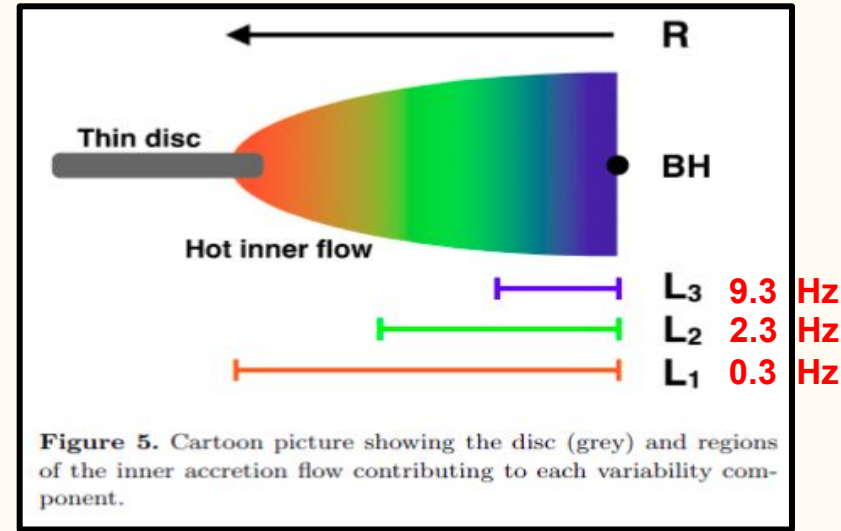
Comparison to observational Data



Pottschmidt et al. (2003)

The corresponding peak frequencies from our time dependent model are: **0.45 Hz, 1.7 Hz, 10.5 Hz, and 35.0 Hz.**

L4 40 Hz
L3 6.0 Hz
L2 2.0 Hz
L1 0.2 Hz



Axelsson & Done (2018)

Some comments on our outcome

- ➡ Our model cannot directly address the issue of the location of the specific emission component since the emissivity properties of the hot medium are not yet included in our model.
- ➡ On the other hand, we follow numerically the flow dynamics so all the aspects of the variability model based on the idea of the propagating fluctuations (Lyubarskii 1997; Kotov et al. 2001; Ingram & Done 2012) are automatically included by us.
- ➡ The model we use is appropriate for black hole accretion due to the specific inner boundary conditions.
- ➡ Our time-dependent evolution of the hot flow does not yet include the interaction with the cold disk which likely overlaps with the hot flow at some range of radii even in the Hard State (e.g. Basak et al. 2017; Zdziarski & De Marco 2020)
- ➡ Out of these all effects, the issue of the angular momentum budget is the most important one for our model since the existence of the shock requires the angular momentum removal to remain in the proper parameter space.

Conclusion

The Lorentzian fitting shows that the hot flow close to the black hole is mostly similar for models with and without wind but the major difference can be seen in the first Lorentzian which represents the oscillations at large radii.

The χ^2 values are high in our models due to very small statistical errors in the high frequency part in the PDS. They are actually dominated by the highest frequency point. Below 100 Hz the deviations in individual bins are of order of 2σ or smaller, very similar to the data residuals shown in Pottschmidt et al. (2003).

Our low-angular momentum coronal accretion model is able to represent the propagation of the perturbation from the outer boundary and explain the variability pattern seen in the Hard State of Cygnus X-1. [arXiv:2009.09121](https://arxiv.org/abs/2009.09121)

